blood®
Regular Article

THROMBOSIS AND HEMOSTASIS

Loss of α4A- and β1-tubulins leads to severe platelet spherocytosis and strongly impairs hemostasis in mice

Quentin Kimmerlin,[1] Sylvie Moog,[1] Alexandra Yakusheva,[1,2] Catherine Ziessel,[1] Anita Eckly,[1] Monique Freund,[1] Gábor Závodszky,[3] Yannick Knapp,[4] Pierre Mangin,[1] and François Lanza[1]

[1]Institut National de la Santé et de la Recherche Médicale, Etablissement Français du Sang Grand Est, Unité Mixte de Recherche-S 1255, Fédération de Médecine Translationnelle de Strasbourg, Université de Strasbourg, Strasbourg, France; [2]Center for Theoretical Problems of Physicochemical Pharmacology, Cellular Hemostasis Lab, Moscow, Russia; [3]Computational Science Lab, Informatics Institute, University of Amsterdam, Amsterdam, The Netherlands; and [4]Avignon University, LAPEC EA4278, Avignon, France

KEY POINTS

- Platelets lacking α4A- and β1-tubulins are devoid of marginal band and fully spherical and inefficiently interact with matrices under flow.
- Mice deficient for α4A- and β1-tubulins exhibit severe defects in hemostatic and thrombotic responses in vivo.

Native circulating blood platelets present with a discoid flat morphology maintained by a submembranous peripheral ring of microtubules, named marginal band. The functional importance of this particular shape is still debated, but it was initially hypothesized to facilitate platelet interaction with the injured vessel wall and to contribute to hemostasis. The importance of the platelet discoid morphology has since been questioned on the absence of clear bleeding tendency in mice lacking the platelet-specific β1-tubulin isotype, which exhibits platelets with a thinner marginal band and an ovoid shape. Here, we generated a mouse model inactivated for β1-tubulin and α4A-tubulin, an α-tubulin isotype strongly enriched in platelets. These mice present with fully spherical platelets completely devoid of a marginal band. In contrast to the single knockouts, the double deletion resulted in a severe bleeding defect in a tail-clipping assay, which was not corrected by increasing the platelet count to normal values by the thrombopoietin-analog romiplostim. In vivo, thrombus formation was almost abolished in a ferric chloride–injury model, with only a thin layer of loosely packed platelets, and mice were protected against death in a model of thromboembolism. In vitro, platelets adhered less efficiently and formed smaller-sized and loosely assembled aggregates when perfused over von Willebrand factor and collagen matrices. In conclusion, this study shows that blood platelets require 2 unique α- and β-tubulin isotypes to acquire their characteristic discoid morphology. Lack of these 2 isotypes has a deleterious effect on flow-dependent aggregate formation and stability, leading to a severe bleeding disorder.

Introduction

Blood platelets are produced by bone marrow megakaryocytes and are essential to arrest and prevent bleeding. In their resting state, platelets harbor a lenticular morphology that is maintained by a submembranous microtubule marginal band.[1] This remarkable structure, which has no equivalent in any other mammalian cell, comprises tightly associated microtubules forming a ring-like structure under the platelet cortex. Despite its identification more than 50 years ago,[2] the formation and functional importance of this architectural singularity has until now escaped full comprehension. To date, several tubulin isotypes have been implicated in the biology of the marginal band: the divergent β1-tubulin and the more generic α4A- and α8-tubulin isotypes. Mutations in these 3 isotypes found in human patients, as well as the genetic ablation of β1-tubulin in mice, result in abnormal platelet and marginal band formation characterized by fewer or scattered microtubules coils. This translates into decreased platelet counts accompanied by an overall loss of their disc-shaped profile in favor of an ovoid morphology.[3-5] As of yet, it is still unclear how the tubulin isotypes participate in these processes, but one can envision that they favor microtubule bending, either directly or indirectly through particular microtubule-associated proteins. Strikingly, although these 3 isotypes are required for efficient platelet formation in mice and humans, they appear on their own to be dispensable for platelet functions.[3-6]

A long-standing hypothesis that remains to be demonstrated is that the flat shape of platelets is important for their hemostatic properties by providing an extended surface, which allows for closer contacts with the exposed matrix upon vascular lesion.[7] This would particularly influence their behavior under the hydrodynamic forces exerted inside the blood vessel. In favor of this hypothesis, but limited to the in vitro setting, it has been observed that spherical human platelets translocated much

faster on a von Willebrand factor (VWF) matrix when compared with their disc-shaped counterparts.[8] This behavior appeared to directly depend on the morphologic differences since cold-treated, fixed spherical platelets behaved similarly. Importantly, however, the spherical shape in these studies does not correspond to a native state but reflects their activation during translocation on VWF or upon cold exposure. Definitive proof for a role of the discoid platelet shape in primary hemostasis requires models in which platelets harbor a spherical shape under native resting conditions. Inducing microtubule depolymerization by low temperature or with tubulin drugs is not suitable for in vivo studies as it alters the platelet native state. A more suitable approach is genetic inactivation of essential platelet tubulin isotypes. β1-tubulin deficient mice (KOB1) represent such a model, in which resting platelets exhibit a lower number of microtubules in their marginal band and a loss of their discoid shape. This morphologic change, however, did not translate into a significant increase in tail bleeding times, which appeared to disprove the biological importance of the platelet discoid morphology.[6] One limitation of this model is that KOB1 platelets still exhibit a thin but tightly assembled marginal band representing ~30% of the normal number of microtubules and adopt an elliptic rather than fully spherical shape.[9] A stronger indication for a hemostatic role of the disc-shape morphology came from the report of a patient presenting with a bleeding diathesis and severe platelet spherocytosis.[10] Remarkably, his platelets were completely devoid of a marginal band and were fully spherical. Although the link between microtubule dysfunctions and bleeding was not formally established, this case raised the hypothesis that spherocytosis could, on its own, impede hemostasis.

In view of phenotype similarities between β1- and α4A-tubulin–mutated patients, and since α- and β-tubulins always work as dimers, we hypothesized that defects in both subunits could amplify the deleterious effect of the single β1 inactivation. In particular, we expected a more severe marginal band defect and complete spherocytosis, which in turn would allow for an accurate determination of the importance of platelet shape in their functions and hemostasis. To this end, we generated *Tuba4a* and *Tubb1* double knockout mice (DKO). In contrast to the single knockouts, the large majority of DKO platelets were fully spherical under resting conditions, and their marginal band was no longer observed. Remarkably, these mice presented a marked bleeding diathesis and near-absent thrombus formation in a ferric chloride ($FeCl_3$) arterial injury model. In vitro flow assays demonstrated an unstable interaction of DKO platelets with a VWF matrix and the formation of smaller and less-compact aggregates on collagen. In line with these results, DKO mice were protected from death in a thromboembolism model. These results strongly support the functional importance of the microtubule-dependent discoid shape in hemostasis and thrombus formation.

Methods

Mice

C57Bl/6 *Tuba4a* knockout mice (KOA4A) were generated at Charles River (Grenoble, France) by CRISPR/Cas9-mediated deletion of exon 2 of the *Tuba4a* gene. They were viable, reproduced normally, and did not express α4A-tubulin (supplemental Figure 1A, available on the *Blood* website). C57Bl/6 *Tubb1* knockout mice (KOB1) were generated by backcrossing mixed Sv129-C57Bl/6 *Tubb1*-deficient mice (kindly provided by Ramesh Shivdasani) with C57Bl/6 mice for 5 generations. C57Bl/6 *Tuba4a* and *Tubb1* double knockout mice (DKO) were obtained by crossbreeding KOA4A and KOB1 knockout mice. For romiplostim-treated animals, mice were administered a single dose (100 μg/kg) 6 days prior to the experiment. Protocols involving animals were performed in accordance with the CREMEAS Committee on the Ethics of Animal Experiments of the University of Strasbourg (Permit Number: E67-482-10).

Tail bleeding assay

Tails of anesthetized 8- to 20-week-old mice were amputated at their distal part by 3 mm and immediately immersed in warm (37°C) 0.9% saline solution. Mice were considered as bleeders until the bleeding stopped for the first time. Bleeding was recorded for 30 minutes, after which it was stopped with hemostatic gauzes if it had not ceased by itself.

Flow experiments

Hirudinated whole blood was perfused into polydimethylsiloxane channels coated with plasma-captured VWF with the VA-IIA-23 peptide (100 μg/mL, Cambcol Laboratories, Cambridgeshire, United Kingdom) or Type I Horm collagen (200 μg/mL, Takeda, Konstanz, Germany).[11] Platelets were visualized using differential interference contrast (DIC) microscopy with an inverted Leica DMI 4000 B microscope (Leica Microsystems, Mannheim, Germany; 40×, 1.4 numerical aperture oil lens). Data were recorded using a complementary metal oxide semiconductor camera (ORCA-Flash4.0 LT, Hamamatsu, Massy, France) and analyzed using ImageJ software (National Institutes of Health).

In vivo thrombosis

$FeCl_3$-induced thrombosis was performed as previously described.[12] Thrombus formation was monitored in real time with a fluorescence microscope (Leica Microsystems) and a charged-couple device camera (CoolSNAP HQ2, Photometrics, Roper Scientific). For scanning electron microscopy, the carotid arteries were fixed with 2.5% glutaraldehyde by transcardiac perfusion and excised within a 120-second time frame. They were subsequently fixed in 2.5% glutaraldehyde, dehydrated, dried, sectioned lengthwise and sputtered with platinum palladium, and examined under a Helios NanoLab dual beam microscope (FEI, Eindhoven, The Netherlands).

Venous thromboembolism

Venous thromboembolism was induced by injecting a mixture of collagen (0.8 mg/kg) and adrenaline (60 μg/kg) in the jugular vein.[13]

Statistical analyses

Results were expressed as the mean (± standard error of the mean [SEM]). Statistical comparisons were performed as described in the figure legends. Normality and equality of variance were evaluated with a Shapiro-Wilk and a Bartlett test, respectively.

Results

Loss of the marginal band in the combined absence of α4A- and β1-tubulins leads to platelet spherocytosis

To evaluate the hypothesis that β1- and α4A-tubulin isotypes cooperate in sustaining platelets' discoid shape, we generated a mouse strain doubly inactivated for these 2 isotypes (DKO) (supplemental Figure 1A). DKO mice had reduced platelet counts and increased volumes (with counts and volumes representing 42% and 153% of those in wild-type [WT] mice, respectively; Figure 1A-B). A similar but less pronounced phenotype was observed in *Tubb1*-deficient mice (KOB1), with counts and volumes representing 66% and 142% of the WT values, respectively. By contrast, single knockout of *Tuba4a* (KOA4A) did not significantly affect platelet counts and sizes. No differences in leukocyte counts, red blood cell counts, and hemoglobin concentration were observed between the 4 strains, showing that the defect is restricted to the platelet lineage (supplemental Figure 1B-D). Apart from the remarkable change in volume, platelets lacking α4A- and β1-tubulins showed profound alterations of shape and ultrastructure. In transmission electron microscopy images, almost all DKO platelets (97%) lacked the typical discoid shape, with 73% appearing as round and 24% as oval (Figure 1C-D). Focused ion beam-scanning electron microscopy analysis illustrated the spherical morphology of DKO platelets and also revealed a slight increase in dense granule density but a normal density of α-granules and mitochondria (supplemental Video 1 and supplemental Figure 2A-C). Transmission electron microscopy examination of KOB1 platelets confirmed the previously reported loss of discoid shape[9] and highlighted that these platelets mostly displayed an ovoid or elliptical shape (68%) rather than a fully round shape (24%). Therefore, the loss of the β1-tubulin isotype alone is less deleterious than the loss of both β1- and α4A-tubulins.

In striking contrast with WT platelets, in which 9 to 12 bundled microtubules were observed in transversal sections, microtubules were very rarely visualized in DKO platelets, and when observed, they appeared as separate entities (supplemental Figure 3A). Fluorescence microscopy observation confirmed the lack of a marginal band in 84% of DKO platelets, which closely matches the proportion of round elements observed in transmission electron microscopy (supplemental Figure 3B). Taken together, the spherical shape of DKO platelets and the profound microtubule deficiency compose a novel and unique phenotype, distinct from that in normal and single tubulin knockout platelets and differing from all known models of macrothrombocytopenia.

One possible cause for the absence of a marginal band in DKO mice could be an insufficient amount of tubulin dimers precluding efficient microtubule growth. Enzyme-linked immunosorbent assay quantification of total α-tubulin indeed revealed a decrease in total tubulin levels in DKO platelets, which represented 38% of those in the WT (Figure 1E). KOB1 platelets also exhibited a decreased content of total α-tubulin (47% of WT levels) but, contrary to the DKO, maintained the ability to assemble a minimal marginal band composed of 3 to 4 microtubules.[9] The additional decrease in tubulin content in DKO platelets is somewhat moderate, but we cannot eliminate the possibility that it reaches subcritical concentrations for microtubule polymerization.

An additional hypothesis to explain the defect is that microtubule assembly is not altered in itself but that platelet microtubules are unstable in the absence of these 2 essential isotypes. To test this hypothesis, DKO platelets were treated with paclitaxel (Taxol) in order to promote microtubule polymerization. Remarkably, microtubules were clearly observed by fluorescence microscopy in 85% of the platelets in paclitaxel-treated platelets compared with only 15% in the untreated DKO control (supplemental Figure 4A-B). A fraction of these microtubule-positive platelets harbored a marginal band-like structure, although the large majority presented a less structured microtubule array. As a control, paclitaxel was also tested on WT, KOA4A, and KOB1 (supplemental Figure 4A). This did not modify microtubule organization in the WT and KOA4A, whereas microtubule labelling appeared more intense and drop shape structures were observed in KOB1. Expression of a number of non-tubulin proteins known to be involved in megakaryopoiesis was additionally evaluated and found to be normal in the DKO, pointing to a tubulin-restricted defect (supplemental Figure 5). Altogether, these results suggest that the lack of visible microtubules in DKO platelets could result from a subcritical tubulin content or unstable microtubules caused by the combined lack of 2 complementary isotypes.

Megakaryocyte maturation and proplatelet extension are severely hampered in the absence of α4A- and β1-tubulins

The low platelet counts in DKO mice could possibly be due to their increased removal from the circulation or a decreased production. Platelet survival curves, generated by in vivo biotinylation, were superimposable to those in the WT mice, demonstrating a normal recirculation (Figure 2A). We then examined whether megakaryopoiesis could be affected. The proportion of bone marrow MEP and MKP progenitors (Figure 2B-C), and the ploidy of $CD42^+$ megakaryocytes (MKs) (supplemental Figure 6A) of DKO mice were similar to those in the WT, KOA4A, and KOB1 mice. On the other hand, the MK density was increased (Figure 2D), and fewer MKs reached the most mature stage (stage III) in DKO compared with WT, KOA4A, and KOB1 as analyzed by transmission electron microscopy of the bone marrow (Figure 2E). In addition, a number of DKO stage III MKs showed defects in their demarcation membrane system (DMS), with tighter membrane contacts and signs of actin accumulation (Figure 2F). This defect was also found in the KOA4A and KOB1 MKs but to a much lesser extent. When MKs were differentiated from bone marrow Lin^- progenitors, large DKO MKs were obtained, which, however, were unable to extend proplatelets, similar to KOB1 MKs (supplemental Figure 6B). In contrast, KOA4A MKs formed proplatelets normally. Therefore, the worsened macrothrombocytopenia of DKO mice when compared with KOB1 could stem from additional megakaryocyte maturation defects.

α4A- and β1-tubulin double deficiency severely impacts hemostasis and thrombus formation

Peritoneal bleeding was noticed in DKO mice upon abdomen incision, an event which was never observed in WT, KOA4A, or KOB1 mice. To explore this further, tail bleeding assays were

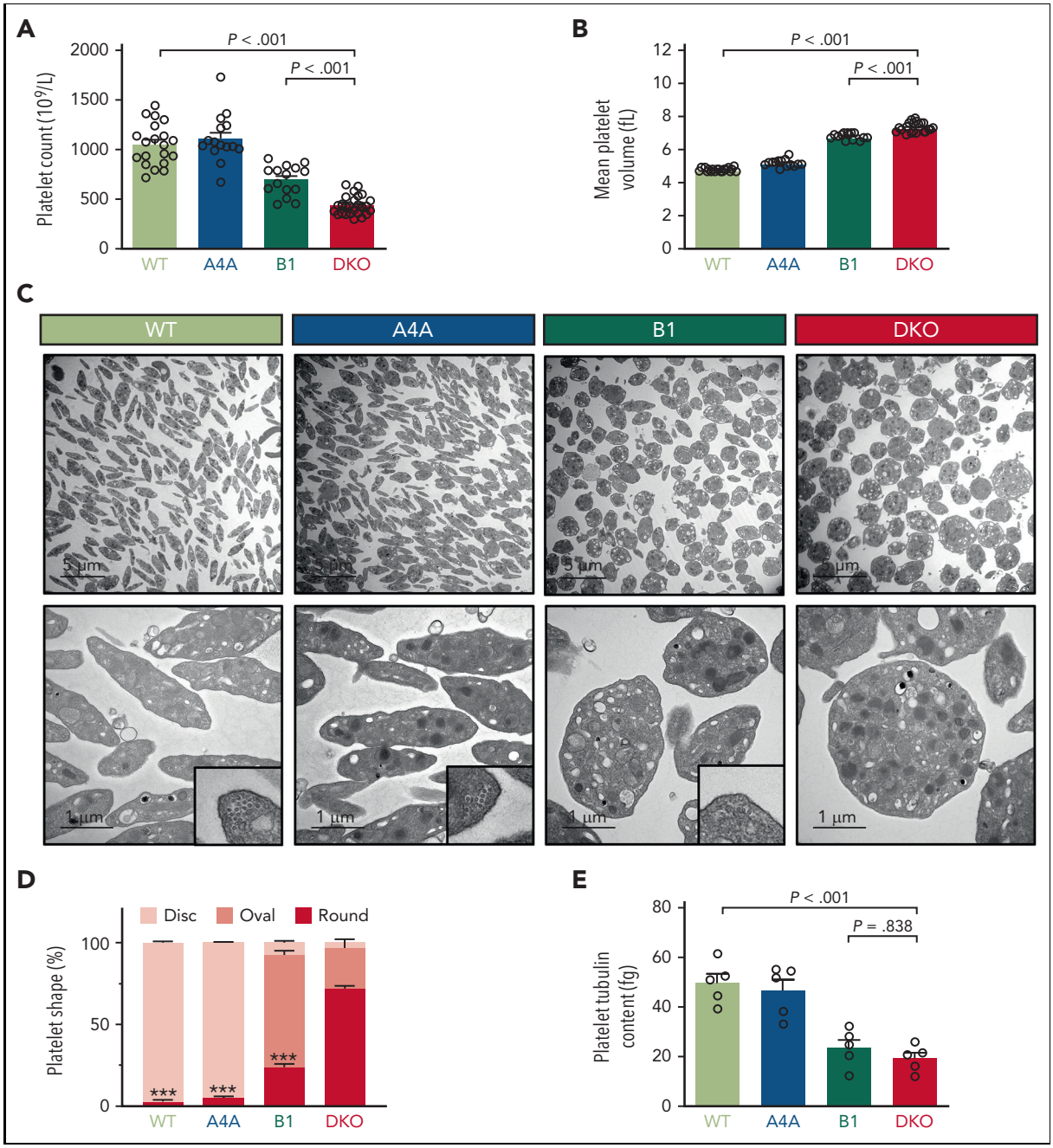

Figure 1. Loss of α4A- and β1-tubulins leads to severe spherocytosis and prevents marginal band formation. (A) Blood platelet counts of WT, KOA4A (A4A), KOB1 (B1), and DKO mice. Results are expressed in 10^9/L. Bar graph represents the mean ±SEM. Each data point corresponds to an individual mouse. N > 20 per strain. Statistical analysis was conducted by 1-way analysis of variance (ANOVA) followed by Tukey honest significant difference (HSD) post-hoc test. (B) Mean platelet volumes of WT, KOA4A (A4A), KOB1 (B1), and DKO mice. Results are expressed in fL. Bar graph represents the mean ±SEM. Each data point corresponds to an individual mouse. Statistical analysis was conducted by Welch ANOVA followed by Dunnett T3 post-hoc test. (C) Representative transmission electron micrographs of WT, KOA4A (A4A), KOB1 (B1), and DKO platelets. The top panels correspond to a large field of view. The lower panels correspond to a close-up view, and higher magnifications in the lower right corners show a cross-sectioned microtubule marginal band for WT, KOA4A, and KOB1 platelets that is absent in DKO platelets. Scale bar: 5 µm (top panel), 1 µm (bottom panel), and 250 nm (lower right corner). (D) Distribution of WT, KOA4A (A4A), KOB1 (B1), and DKO platelets according to their morphology. Platelets were manually ranked based on their morphology (disc, oval, or round). Results are expressed in % of each class. Bar graph (stacked) represents the mean ±SEM, with at least >100 platelets per genotype counted. Statistical analysis of the round morphology was conducted by 1-way ANOVA followed by Tukey HSD post-hoc test, with DKO as a reference. ***$P < .001$. (E) Enzyme-linked immunosorbent assay quantification of total tubulin of platelet lysates of WT, KOA4A (A4A), KOB1 (B1), and DKO mice. Results are expressed in fg per platelet. Bar graph represents the mean ±SEM. Each data point corresponds to an individual platelet lysate, obtained from a single mouse. N > 3 per group. Statistical analysis was conducted by 1-way ANOVA followed by Tukey HSD post-hoc test.

performed, which revealed a marked bleeding tendency in DKO compared with WT mice, with a majority of DKO mice (71%) still bleeding 30 minutes after injury, in comparison with 6% of WT, 16% of KOA4A, and 33% of KOB1 mice (Figure 3A). A possible reason for the increased bleeding severity in DKO could be their low platelet count. To evaluate this, DKO mice

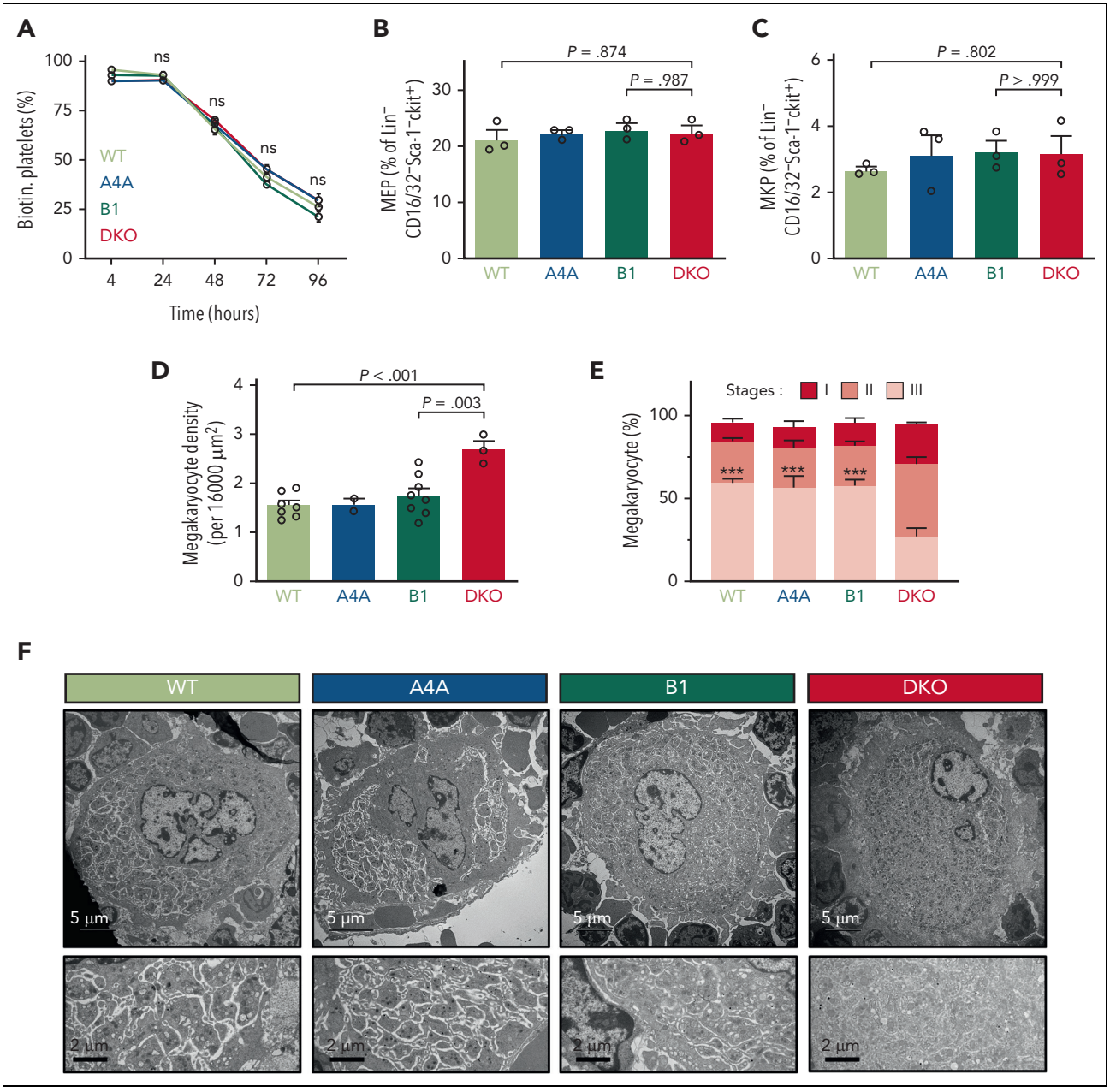

Figure 2. Megakaryopoiesis is severely hampered in the absence of α4A- and β1-tubulins. (A) Flow cytometry analysis of platelet survival by in vivo biotinylation in WT, KOA4A (A4A), KOB1 (B1), and DKO mice. Graph represents the proportion over time of circulating biotin-labelled platelets. Results are expressed in %. Each symbol represents the mean ±SEM. N = 4 for each strain. Statistical analysis was conducted by 1-way ANOVA followed by Tukey HSD post-hoc test (not significant [ns]: $P > .05$). (B-C) Flow cytometry analysis of (B) megakaryocyte/erythroid progenitor (MEP) (Lin^- $CD16/32^-$ $Sca\text{-}1^-$ $ckit^+$ $CD150^+$ CD9dim) and (C) megakaryocyte progenitor (MKP) (Lin^- $CD16/32^-$ $Sca\text{-}1^-$ $ckit^+$ $CD150^+$ CD9bright) populations in freshly isolated, lineage-depleted bone marrow cell suspensions from WT, KOA4A (A4A), KOB1 (B1), and DKO mice. Results are expressed as % of the Lin^- $CD16/32^-$ $Sca\text{-}1^-$ $ckit^+$ cell population. Bar graphs represent the mean ±SEM. Each data point corresponds to an individual experiment. N = 3. Statistical analysis was conducted by 1-way ANOVA followed by Tukey HSD post-hoc test. (D) Megakaryocytes were manually counted from transmission electron micrographs of bone marrow sections of WT, KOA4A (A4A), KOB1 (B1), and DKO mice. Results are expressed as number of megakaryocytes per unit of surface (16 000 $µm^2$). Bar graph represents the mean ±SEM. Each data point corresponds to an individual mouse. Statistical analysis was conducted by 1-way ANOVA followed by Tukey HSD post-hoc test. (E) Megakaryocytes from WT, KOA4A (A4A), KOB1 (B1), and DKO mice were manually classified (stages I, II, and III) based on morphologic criteria, evaluated from transmission electron micrographs of bone marrow sections. Results are expressed as % of each class. Stacked bar graph represents the mean ±SEM. N = 3 with at least 30 megakaryocytes counted per preparation. Statistical analysis of the stage III megakaryocytes was conducted by 1-way ANOVA followed by Tukey HSD post-hoc test, with DKO as a reference. ***$P < .001$. (F) Representative transmission electron micrographs of stage III megakaryocytes observed in bone marrow sections of WT, KOA4A (A4A), KOB1 (B1), and DKO mice. Bottom panels show close-up views of the demarcation membrane system. Scale bar, 5 µm (top panels) and 2 µm (bottom panels).

were treated with the thrombopoietin-analog romiplostim to increase their platelet counts without modifying the platelet volume (supplemental Figure 7A-B), a treatment which was adapted to preserve the expression of key surface glycoproteins, including the collagen receptor GPVI, and normal activation (supplemental Figure 7C-D). Under these conditions, there was no improvement of the bleeding diathesis, despite platelet counts reaching WT levels (Figure 3A).

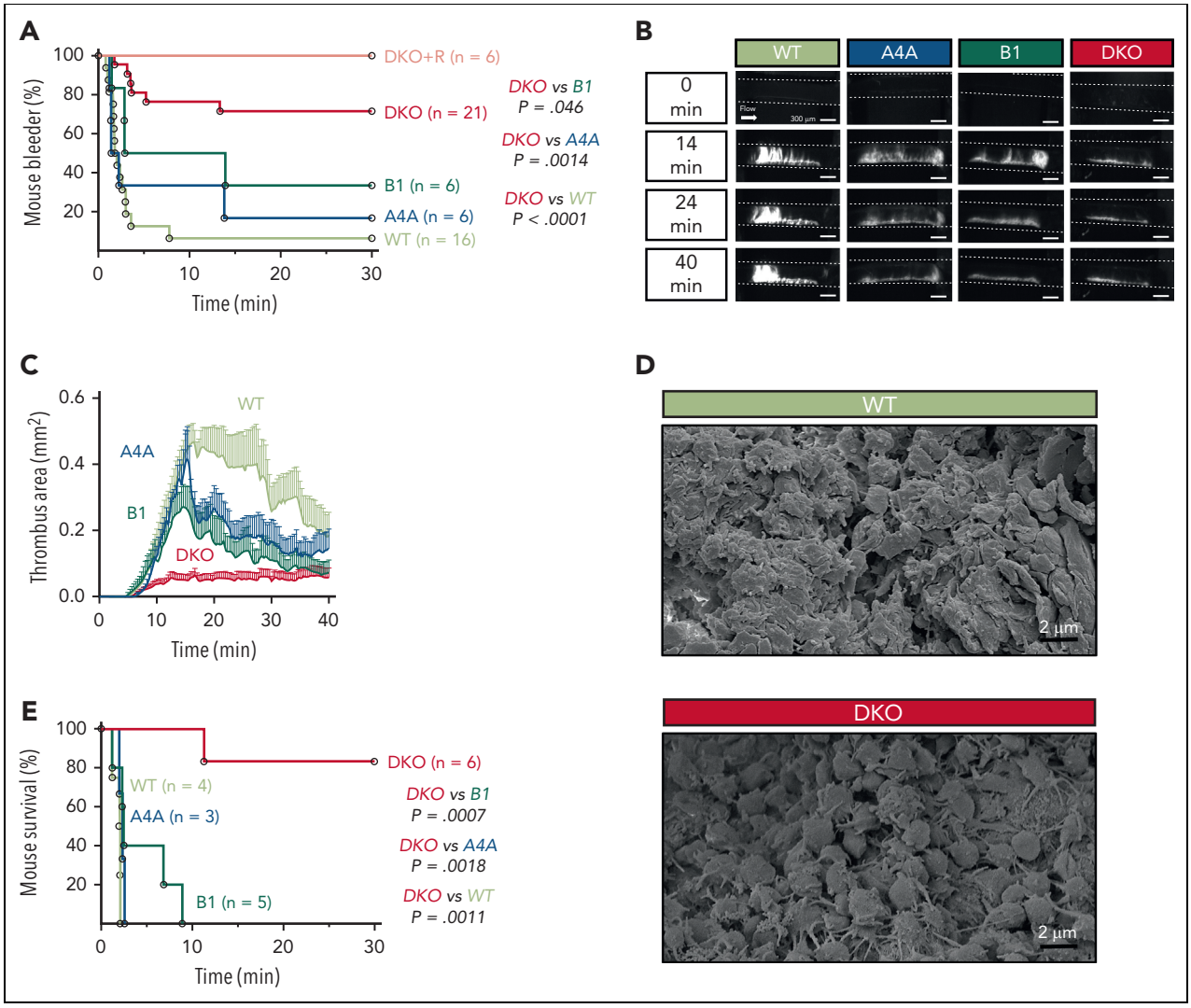

Figure 3. Loss of α4A- and β1-tubulins severely impairs hemostatic and thrombotic responses in vivo. (A) Percentage of bleeders over time following a 3-mm tail-tip amputation for WT, KOA4A (A4A), KOB1 (B1), and DKO mice and romiplostim-treated DKO mice (DKO+R). Results are represented as Kaplan-Meier survival curves. For romiplostim-treated animals, mice were administered a single dose (100 µg/kg) 6 days prior to the experiment. N > 6 per group. Statistical analysis was conducted by the log-rank test. (B) Representative fluorescence micrographs of thrombi formed at 14, 24, and 40 minutes after topical application of $FeCl_3$ to the carotid artery of WT, KOA4A (A4A), KOB1 (B1), and DKO mice. Platelets were labeled by 3,3′-dihexyloxacarbocyanine iodide injection. (C) Thrombus area quantification after topical application of $FeCl_3$ to the carotid artery of WT, KOA4A (A4A), KOB1 (B1), and DKO mice. Results are expressed in mm^2 as a function of time (minutes). N > 5 per strain. (D) Representative scanning electron micrographs of WT and DKO thrombi in transsectioned carotid arteries that have been fixed 7 minutes after topical application of $FeCl_3$. (E) Percentage of survival over time of WT, KOA4A (A4A), KOB1 (B1), and DKO mice in a venous thromboembolism model following an injection in the jugular vein of a mixture of collagen (0.8 mg/kg) and adrenaline (60 µg/kg). Results are represented as Kaplan-Meier survival curves. N > 3 per group. Statistical analysis was conducted by the log-rank test. Scale bars, 300 µm (B) and 2 µm (D).

We then asked whether the hemostatic defect would be accompanied by a decreased capacity to form a thrombus in vivo. In a carotid $FeCl_3$-injury model, which combines high shear rate conditions and a damage to the endothelium,[14] only a thin layer of platelets accumulated at the site of lesion in DKO, whereas thrombi progressively grew to almost occlude the artery in WT mice (Figure 3B). At its maximum, DKO thrombus size only represented 14% of that in WT animals (Figure 3C and supplemental Figure 8). Close examination at the injury site by scanning electron microscopy revealed that the inner wall of the vessel was unevenly covered by platelets in DKO mice, leaving most areas with only a few layers of platelets and devoid of major aggregates. Close-up views showed that these platelets were loosely packed and appeared as spherical elements extending filopodia (Figure 3D). In contrast, the thrombus was voluminous in the WT, showing densely packed platelets in its center and loosely aggregated discoid platelets at the outer surface, in agreement with the previously described core/shell architecture of these thrombi.[15] Thrombus formation in KOA4A and KOB1 mice differed from that in DKO, since it reached a maximal surface close to that in WT with, however, a tendency towards faster resorption.

In view of the loose aspect of the thrombi in the DKO, we next examined whether these mice would have a lower tendency to occlude their microcirculation in a model of thromboembolism induced by a jugular injection of a mixture of collagen and adrenaline. Whereas the WT and single knockout mice all died rapidly after injection, DKO mice were protected against death, with 83% survivors during a 30-minute observation period (Figure 3E).

Decreased flow-dependent adhesion and aggregation

Abnormal hemostasis and thrombosis in DKO mice could originate from defective platelet activation responses. At a resting state, the major platelet glycoproteins (corrected for the platelet surface) were not decreased in DKO platelets (supplemental Figure 9A). P-selectin exposure (which reflects α-granule release) and serotonin secretion (which reflects δ-granule release) remained comparable to those in WT in response to a range of concentrations of thrombin or CRP and thrombin or collagen, respectively (supplemental Figure 9B-C). Similarly, platelet aggregation in a turbidimetric assay was not decreased but rather slightly increased in DKO mice following activation by ADP, thrombin, or collagen (supplemental Figure 10) and collagen + adrenaline stimulation (supplemental Figure 11), thus questioning an intrinsic defect in intracellular signaling under the low shear conditions of these types of assays. The preserved ability of DKO platelets to interact in the aggregometer suggested that, in vivo, these platelets could incorporate within a thrombus forming in WT mice. This was indeed observed when fluorescently labelled DKO platelets were transfused into WT mice before $FeCl_3$-injury of the carotid artery (supplemental Figure 12). Finally, adhesion assays were performed on fibrinogen and collagen matrices in which increased spreading was observed for DKO platelets and to a lesser extent for TUBB1 platelets (supplemental Figure 13). The significance of this increased response for the hemostatic and thrombosis defects is open to question in view of the disputed role of platelet spreading on thrombus formation.[16]

The primary event in platelet plug formation in vivo is their shear-dependent interaction with VWF that could be affected by the abnormal platelet shape in DKO. To explore this, we performed blood perfusion studies in microchannels coated with a VWF-binding antibody, which allows for VWF capture directly from the blood that is perfused in the microfluidic device. Care was taken to confirm equal levels of plasma VWF in DKO mice (supplemental Figure 14) and to allow a slight delay before recording the videos to ensure the proper capture of the plasma VWF. In this assay, whereas WT and KOA4A platelets adopted a sliding or flip-flop mode of displacement, KOB1 and DKO platelets rolled over the VWF matrix. This occurred at a much higher speed for DKO platelets compared with KOB1, KOA4A, and WT platelets (Figure 4A-D). In addition, DKO platelets were more easily detached from the matrix when compared with KOB1 (Figure 4E-F). Interestingly, this abnormal interaction was observed at both high (3000 s^{-1}) and low (500 s^{-1}) shear rates, suggesting that it could affect hemostasis equally in the arteries and veins.

Additional flow-dependent defects were explored upon exposure to the more reactive collagen matrix, which results in the formation of platelet thrombi upon perfusion of WT blood. Time-course analyses revealed a delay in thrombus buildup when DKO blood was perfused and a significant decrease in the surface area occupied by platelets representing 66% of that in WT at 1.75 minutes (Figure 5A-B). Similar results were obtained when the platelet count was brought to normal values by romiplostim administration, indicating that formation of smaller thrombi was not due to the lower platelet count. Altogether, these results strongly suggest that the abnormal platelet shape is an important contributor of the hemostatic defects in DKO mice.

Discussion

Of all the blood cellular components, platelets uniquely exhibit a very small size and a discoid shape maintained by the microtubule marginal band. This flat morphology endows platelets particular hydrodynamic properties and has long been hypothesized to contribute to hemostasis. The hypothesis, however, has been questioned when KOB1 mice showed no major bleeding tendency despite presenting with platelets lacking the typical disc-shaped morphology. Nonetheless, these results do not fully disprove the original theory, since KOB1 platelets still exhibit a residual marginal band composed of 2 to 3 microtubules, leaving their platelets ovoid rather than fully spherical.[9] Here, we have generated a mouse model doubly inactivated for β1- and α4A-tubulins, which presents macrothrombocytopenia with an unprecedented degree of platelet spherocytosis due to a complete lack of marginal band. Interestingly, the double deletion had a profound negative impact on hemostatic and thrombotic responses in vivo. This could not be attributed to an overall decrease in platelet reactivity but was more likely caused by inefficient matrix interaction and an impaired capacity to form cohesive aggregates under hemodynamic conditions.

Presently, the role of microtubules in platelet biogenesis remains poorly defined. In view of the abnormal DMS of DKO megakaryocytes, it becomes clear that this cytoskeleton is involved in some way in the generation of this structure. Microtubules are known to play a role in cargo transport from the Golgi complex.[17,18] This opens the possibility of similar functions for DMS formation, which is fueled from the plasma membrane and also from the Golgi apparatus.[19] The other clear evidence from this DKO model is that α4A- and β1-tubulins functionally cooperate to assemble the platelet marginal band. Their exact contribution to this process remains, however, unclear. Knowing that growing microtubules have been observed in circulating platelets, it is likely that tubulin polymerization might take part in marginal band formation in vivo.[20] Therefore, the quantitative deficit in total tubulin of DKO platelets could well result in suboptimal concentrations that may prevent proper microtubule polymerization. Another hypothesis to explain the lack of marginal band in DKO platelets is that microtubules lacking the β1- and α4A-tubulins may be less amenable to bend and to form such structure. This hypothesis is supported by the fact that β1-tubulin was shown to induce bends in CHO cells[21] and that microtubule buckling in muscle cells is reduced when tubulin tyrosination levels are increased,[22] such as when the naturally detyrosinated α4A-tubulin isotype is missing.[4] Altogether, the combination of reduced tubulin content and the potential inability of microtubules to curve could account for the absence of marginal band in DKO platelets. In agreement with this, the microtubule agent paclitaxel, which stabilizes growing microtubule and decreases their flexural rigidity,[23] partially restores this phenotype. At variance with the macrothrombocytopenia observed in the *Tuba4a* V260E mutant mice,[4] *Tuba4a* knockout mice presented with near-normal platelet counts and volumes. This could be due to compensation by other α-tubulins, whereas the mutated

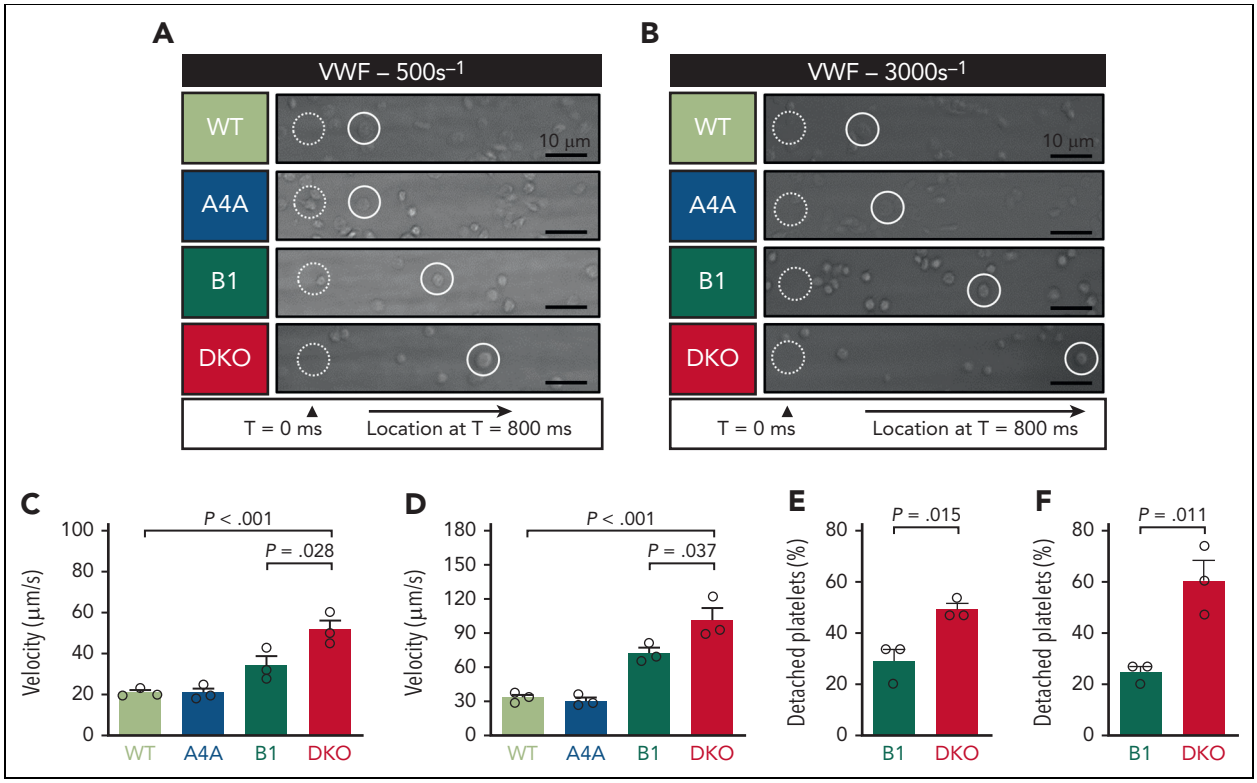

Figure 4. Platelet adhesion onto VWF under flow is reduced in the absence of α4A- and β1-tubulins. (A-B) Representative differential interference contrast (DIC) micrographs of WT, KOA4A (A4A), KOB1 (B1), and DKO platelets rolling onto captured VWF at (A) 500 and (B) 3000 reciprocal seconds (s^{-1}). Hirudinated whole blood was perfused into polydimethylsiloxane channels coated with the VWF-capturing peptide (vA3-III-23, 100 µg/mL). Blood was allowed to flow for 15 seconds before recording videos. For each micrograph, the dotted white circle indicates the initial position of 1 platelet, and the full white circle indicates its position after 800 ms. Scale bar: 10 µm. (C-D) Rolling velocity of WT, KOA4A (A4A), KOB1 (B1), and DKO platelets onto captured VWF at (C) 500 and (D) 3000 reciprocal seconds (s^{-1}). Velocities are expressed as µm/s and were determined based on DIC recordings. Bar graphs represent the mean ±SEM. Each symbol indicates an individual flow. N = 3 per strain, with ≥15 platelets counted per individual flow. Statistical analysis was conducted by 1-way ANOVA followed by Tukey HSD post-hoc test. (E-F) Platelet detachment from the VWF surface at (E) 500 and (F) 3000 reciprocal seconds (s^{-1}) was determined by tracking individual KOB1 (B1) and DKO platelets during 30 seconds on DIC recordings. Results are expressed in %. Bar graphs represent the mean ±SEM. Each symbol indicates an individual flow. N = 3 per strain, with ≥15 platelets counted per individual flow. Statistical analysis was conducted by unpaired 2-tailed *t* test.

form could have a dominant effect through its misincorporation in microtubules.

Round platelets can be obtained by chemical treatment or cold exposure to depolymerize their marginal band, but this occurs at the expense of their activation and uncontrolled cytoskeletal modifications, thereby preventing proper evaluation of the discoid shape in platelet functions. Here, our genetic approach allowed us to circumvent these limitations and provided an ideal model to explore this question. Despite their profound spherocytosis and the lack of marginal band, DKO platelets presented no other structural anomaly and did not exhibit signs of activation at rest, and their responses to the examined agonists were well preserved. Therefore, the marked bleeding tendency observed in DKO mice represents the strongest evidence to date that the native platelet discoid shape sustained by its microtubule scaffold is required for normal hemostasis, supporting a long-standing proposal in the field. Such a severe bleeding stands out from previous mouse models with tubulin deficiencies and is usually observed only when platelets are missing essential platelet receptors such as integrin αIIbβ3 or GPIb-IX or in the occurrence of a profound thrombocytopenia.[24-26] Arguably, DKO mice have a decreased platelet count, but it still represents 42% of that in WT mice. This level is well above the reported threshold of 100 to 25.10^9 platelets/L (~10% to 2.5% of WT) for bleeding occurrence in mice.[26] More importantly, bleeding was still observed when the platelet count of DKO mice was brought to normal levels. Moreover, KOB1 mice, which are also moderately thrombocytopenic (65% of WT), did not exhibit a severe bleeding. Altogether, these results strongly support the notion that the bleeding deficiency in DKO mice is largely influenced by the abnormal platelet shape provided by the absence of a supportive microtubule cytoskeleton.

In addition to increased bleeding, DKO mice also exhibit a major defect in thrombus formation in a classic $FeCl_3$ arterial-injury model. Remarkably, thrombus buildup was nearly abrogated, resembling the most severe defects observed in the absence of essential platelet receptors such as GPIb-IX, integrin αIIbβ3, or P2Y12.[24,27,28] Here again, the low platelet count is not expected to play a major role since thrombus formation is only severely impaired when platelet counts reach ~10% of normal levels in a carotid artery $FeCl_3$-injury model.[26] In addition, the possibility of a vessel-related defect in the observed in vivo phenotypes seems very unlikely since WT mice transplanted with DKO hematopoietic progenitors also exhibited smaller-size thrombi compared with WT mice transplanted with

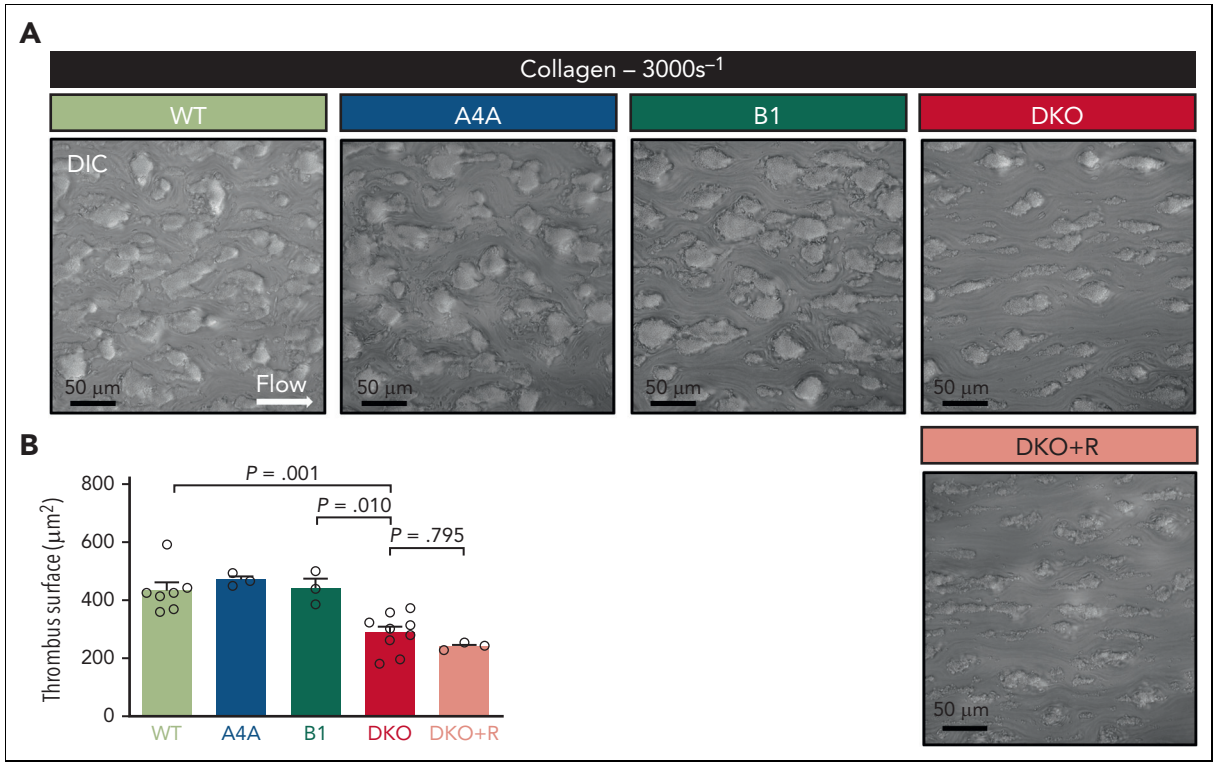

Figure 5. Platelet aggregates formation onto type I collagen matrices under flow is impaired in the absence of α4A- and β1-tubulins. (A) Representative DIC micrographs of aggregates formed after perfusion of hirudinated blood of WT, KOA4A (A4A), KOB1 (B1), DKO, and romiplostim-treated DKO (DKO+R) mice for 105 seconds at 3000 reciprocal seconds (s^{-1}) into type-I collagen-coated (200 µg/mL) polydimethylsiloxane channels. Scale bar, 50 µm. (B) Bar graph representing the mean surface ±SEM of WT, KOA4A (A4A), KOB1 (B1), and DKO mice and romiplostim-treated DKO aggregates formed under the same condition. Results are expressed in $µm^2$. Each symbol indicates an individual flow. N ≥ 3 per group, with at least 250 aggregates counted per individual flow. Statistical analysis was conducted by 1-way ANOVA followed by Tukey HSD post-hoc test.

WT progenitors (supplemental Figure 15). In DKO, the thrombi remained of small size even at late observation times, indicating that inefficient platelet accretion was not simply due to a delayed process. Rather, this suggested that the spherical shape of the platelets is hampering either their margination by erythrocytes or their interaction with the injured vessel and the initially attached platelets. Numerical simulations (supplemental Figure 16) predict similar margination capacity for WT and DKO platelets towards the cell-free layer. Therefore, spherocytosis on its own is not expected to significantly affect margination, which is equally not influenced by the erythrocyte count that is equivalent to WT levels. However, once inside the cell-free layer, their dynamics diverge. The difference in shapes results in significantly higher lift and drag forces on the spherical DKO platelets, which effectively reduce their time availability and thus the chance for binding at the wall.

Flow experiments on VWF, which explore in vitro the first stage of platelet interaction with the exposed subendothelium, revealed higher translocation speeds and easier detachment of DKO platelets. This behavior has been previously observed in VWF flow studies of normal human platelets on their spherical transformation during high-shear perfusion, reflecting an active state.[8] In our study, perfusion was initiated with spherical platelets at a resting state, and their interaction defect was observed at high and low shear rates. Flow studies on a collagen matrix at high shear, corresponding to those of the carotid artery,[29] further revealed formation of smaller aggregates in the DKO, reminiscent of the observations in the $FeCl_3$ thrombosis model. Altogether, the in vitro flow studies indicate that the lack of a microtubule network and associated sphericity result in a combined deficiency in platelet attachment to the matrix and thrombus buildup. A plausible explanation for the resistance to death in DKO mice is that friable aggregates are more easily cleared under the high-shear conditions of the pulmonary microcirculation. It is noteworthy that platelet deformability, which has not been investigated here, could also be modified in the absence of a marginal band and therefore influence platelet behavior under flow.[30]

In conclusion, our study presents the strongest evidence to date that the discoid shape of blood platelets is more than an accessory attribute but is perfectly suited to favor interaction with the injured vessel wall and that its absence drastically hinders hemostasis. One open question at this stage is whether spherocytosis could also impact non-hemostatic functions of platelets.

Acknowledgments

The authors warmly thank Carsten Janke for the excellent discussions and critical review of the manuscript, Ketty Knez-Hippert for her valuable advices on animal welfare and management, and Jean-Yves Rinckel and Fabienne Proamer for their exceptional technical expertise in electron microscopy. The authors also thank Juliette Mulvihill for reviewing the English of the manuscript.

This work was supported by the University of Strasbourg and by the Fondation pour la Recherche Médicale (grant FDT202106013085) (Q.K.).

Authorship

Contribution: Q.K. performed animal experimentation and platelet and megakaryocyte studies, analyzed the data, and cowrote the article; S.M. performed animal experimentation and platelet and megakaryocyte studies and analyzed the data; C.Z. and A.Y. performed animal experimentation; A.E. performed and analyzed electron microscopy imaging; M.F. took care of the animals and performed animal experimentation; G.Z. performed computational simulations and discussed and analyzed the biophysical data; Y.K. discussed the results and analyzed the biophysical data; P.M. discussed the results and analyzed the data; and F.L. designed the study, analyzed the data, and wrote the article.

Conflict-of-interest disclosure: The authors declare no competing financial interests.

ORCID profiles: Q.K., 0000-0002-1999-782X; A.Y., 0000-0001-5292-2312; A.E., 0000-0001-9620-4961; M.F., 0000-0003-2128-8114; G.Z., 0000-0003-0150-0229; Y.K., 0000-0003-3721-4806; P.M., 0000-0001-9522-6261.

Correspondence: François Lanza, UMR_S1255, EFS-Grand Est site de Strasbourg, 10 rue Spielmann, F-67065 Strasbourg Cedex, France; email: francois.lanza@efs.sante.fr.

Footnotes

Submitted 27 April 2022; accepted 16 August 2022; prepublished online on *Blood* First Edition 26 August 2022. https://doi.org/10.1182/blood.2022016729.

For any question regarding materials and methods, contact the corresponding author, François Lanza, via email: francois.lanza@efs.sante.fr.

The online version of this article contains a data supplement.

There is a *Blood* Commentary on this article in this issue.

The publication costs of this article were defrayed in part by page charge payment. Therefore, and solely to indicate this fact, this article is hereby marked "advertisement" in accordance with 18 USC section 1734.

REFERENCES

1. White JG, Rao GHR. Microtubule coils versus the surface membrane cytoskeleton in maintenance and restoration of platelet discoid shape. *Am J Pathol*. 1998;152(2):597-609.
2. Behnke O. Further studies on microtubules. A marginal bundle in human and rat thrombocytes. *J Ultrastruct Res*. 1965;13(5):469-477.
3. Burley K, Westbury SK, Mumford AD. TUBB1 variants and human platelet traits. *Platelets*. 2018;29(2):209-211.
4. Strassel C, Magiera MM, Dupuis A, et al. An essential role for α4A-tubulin in platelet biogenesis. *Life Sci Alliance*. 2019;2(1):e201900309.
5. Kimmerlin Q, Dupuis A, Bodakuntla S, et al. Mutations in the most divergent α-tubulin isotype, α8-tubulin, cause defective platelet biogenesis. *J Thromb Haemostasis*. 2022;20(2):461-469.
6. Italiano JE, Bergmeier W, Tiwari S, et al. Mechanisms and implications of platelet discoid shape. *Blood*. 2003;101(12):4789-4796.
7. Mody NA, Lomakin O, Doggett TA, Diacovo TG, King MR. Mechanics of transient platelet adhesion to von Willebrand factor under flow. *Biophys J*. 2005;88(2):1432-1443.
8. Maxwell MJ, Dopheide SM, Turner SJ, Jackson SP. Shear induces a unique series of morphological changes in translocating platelets: effects of morphology on translocation dynamics. *Arterioscler Thromb Vasc Biol*. 2006;26(3):663-669.
9. Schwer HD, Lecine P, Tiwari S, et al. A lineage-restricted and divergent beta-tubulin isoform is essential for the biogenesis, structure and function of blood platelets. *Curr Biol*. 2001;11(8):579-586.
10. White JG, de Alarcon PA. Platelet spherocytosis: a new bleeding disorder. *Am J Hematol*. 2002;70(2):158-166.
11. Receveur N, Nechipurenko D, Knapp Y, et al. Shear rate gradients promote a bi-phasic thrombus formation on weak adhesive proteins, such as fibrinogen in a VWF-dependent manner. *Haematologica*. 2020;105(10):2471-2483.
12. Janus-Bell E, Yakusheva A, Scandola C, et al. Characterization of the role of integrin α5β1 in platelet function, hemostasis, and experimental thrombosis. *Thromb Haemost*. 2022;122(5):767-776.
13. Léon C, Freund M, Ravanat C, et al. Key role of the P2Y(1) receptor in tissue factor-induced thrombin-dependent acute thromboembolism: studies in P2Y(1)-knockout mice and mice treated with a P2Y(1) antagonist. *Circulation*. 2001;103(5):718-723.
14. Grover SP, Mackman N. How useful are ferric chloride models of arterial thrombosis? *Platelets*. 2020;31(4):432-438.
15. Stalker TJ, Traxler EA, Wu J, et al. Hierarchical organization in the hemostatic response and its relationship to the platelet-signaling network. *Blood*. 2013;121(10):1875-1885.
16. Schurr Y, Sperr A, Volz J, et al. Platelet lamellipodium formation is not required for thrombus formation and stability. *Blood*. 2019;134(25):2318-2329.
17. Hao H, Niu J, Xue B, et al. Golgi-associated microtubules are fast cargo tracks and required for persistent cell migration. *EMBO Rep*. 2020;21(3):e48385.
18. Fourriere L, Jimenez AJ, Perez F, Boncompain G. The role of microtubules in secretory protein transport. *J Cell Sci*. 2020;133(2):jcs237016.
19. Eckly A, Heijnen H, Pertuy F, et al. Biogenesis of the demarcation membrane system (DMS) in megakaryocytes. *Blood*. 2014;123(6):921-930.
20. Patel-Hett S, Richardson JL, Schulze H, et al. Visualization of microtubule growth in living platelets reveals a dynamic marginal band with multiple microtubules. *Blood*. 2008;111(9):4605-4616.
21. Yang H, Ganguly A, Yin S, Cabral F. Megakaryocyte lineage-specific class VI β-tubulin suppresses microtubule dynamics, fragments microtubules, and blocks cell division. *Cytoskeleton (Hoboken)*. 2011;68(3):175-187.
22. Robison P, Caporizzo MA, Ahmadzadeh H, et al. Detyrosinated microtubules buckle and bear load in contracting cardiomyocytes. *Science*. 2016;352(6284):aaf0659.
23. Mitra A, Sept D. Taxol allosterically alters the dynamics of the tubulin dimer and increases the flexibility of microtubules. *Biophys J*. 2008;95(7):3252-3258.
24. Strassel C, Nonne C, Eckly A, et al. Decreased thrombotic tendency in mouse models of the Bernard-Soulier syndrome. *Arterioscler Thromb Vasc Biol*. 2007;27(1):241-247.
25. Hodivala-Dilke KM, McHugh KP, Tsakiris DA, et al. Beta3-integrin-deficient mice are a model for Glanzmann thrombasthenia showing placental defects and reduced survival. *J Clin Invest*. 1999;103(2):229-238.
26. Morowski M, Vögtle T, Kraft P, et al. Only severe thrombocytopenia results in bleeding and defective thrombus formation in mice. *Blood*. 2013;121(24):4938-4947.
27. Evans DJW, Jackman LE, Chamberlain J, et al. Platelet P2Y(12) receptor influences the vessel wall response to arterial injury and thrombosis. *Circulation*. 2009;119(1):116-122.
28. Eckly A, Hechler B, Freund M, et al. Mechanisms underlying $FeCl_3$-induced arterial thrombosis. *J Thromb Haemostasis*. 2011;9(4):779-789.
29. Panteleev MA, Korin N, Reesink KD, et al. Wall shear rates in human and mouse arteries: Standardization of hemodynamics for in vitro blood flow assays: communication from the ISTH SSC subcommittee on biorheology. *J Thromb Haemostasis*. 2021;19(2):588-595.
30. Baumann J, Sachs L, Otto O, et al. Reduced platelet forces underlie impaired hemostasis in mouse models of MYH9-related disease. *Sci Adv*. 2022;8(20):eabn2627.